International Journal of Pharmaceutical Drug Design (IJPDD)
Website: https://ijpdd.org/
ISSN: 2584-2897
Vol. 2, Issue 12, December, 2025
Page No.: 01-25

Research

Design and Characterization of Herbal Nanoemulsion for Topical Therapy of Psoriasis

Abhay Pundir*, Mukesh Kumar, Robin Singh

Department of Pharmacy, IIMT College of Medical Sciences, IIMT University, O-Pocket, Ganganagar, Meerut, 250001, U.P., India

Corresponding Author:
Abhay Pundir

Email:
abhaypundir363@gmail.com, mukeshkmr681@gmail.com, rxrobin1712@gmail.com

DOI: *10.62896/ijpdd.2.12.01*

Conflict of interest: *NIL*

Article History
Received: 12/11/2025
Accepted: 28/11/2025
Published: 01/12/2025

Abstract:
This study focuses on the comprehensive physical characterization, identification, and nanoemulsion formulation of garlic and cinnamon extracts to enhance cutaneous dispersion. A physical investigation revealed that garlic was an off-white powder with a pungent aroma and taste, whereas cinnamon was a reddish-brown powder lacking a distinct form, exuding a sweet and woody scent. The melting point test confirmed the published values: garlic melted at 165°C and cinnamon melted at −7°C. FTIR spectroscopy showed obvious, distinct peaks when it was used to find functional groups. This supports the idea that the molecule is real. The UV spectrophotometric calibration curves in methanol indicated that both extracts had extremely great linearity (R^2 > 0.997). This suggested that the method was good for quantitative analysis. We used oleic acid as the oil phase, Tween 80 as the surfactant, and PEG 400 as the co-surfactant to make nanoemulsions. We accomplished this by analyzing solubility profiles and constructing a pseudo-ternary phase diagram. Out of all the Smix ratios that were tried, the 2:1 ratio made the best nanoemulsion area. Thermodynamic stability tests indicated that formulation A2 has the optimum physicochemical qualities for application on the skin. These were the droplet size (50.00±1.57 nm), the low PDI (0.14±0.03), the pH (6.5±0.52), the viscosity (140.8±3.02 cP), and the high transmittance (97.56±0.06%). Transmission electron microscopy (TEM) confirmed the existence of uniform, spherical nanodroplets free from aggregation. *Ex-vivo* permeation studies employing porcine ear skin demonstrated significantly enhanced penetration and dermal deposition with the nanoemulsion hydrogel (Formulation A2) relative to the conventional carbopol gel, yielding enhancement ratios of 2.93 and 2.74 for garlic and cinnamon, respectively. Stability studies under ICH conditions showed that the droplet size and other physical characteristics didn't change significantly over 90 days. This showed that the formulation was strong.

Keywords: garlic, cinnamon extracts, nanoemulsion, psoriasis

1. Introduction

Psoriasis is an immune-mediated inflammatory condition that is chronic in nature and affects the skin mainly but other structures including the joints, bones, tendons, ligaments, nails, and mucous membranes also get affected. It affects about 79.7 million people worldwide, accounting for 2–4% of the population. Psoriasis ranges from very mild to very severe, varying from red, scaly patches to widespread involvement of all parts of the body (1). Psoriasis usually presents with characteristic skin lesions, typically plaques—well-defined,

erythematous erythematous patches covered with silver-white scales. Plaque elevation is caused by keratinocyte hyperproliferation and a hidden inflammatory reaction. Histopathological assessment of psoriatic plaques shows several characteristic features based on immune dysregulation. The accelerated and premature proliferation of keratinocytes (KCs) causes faulty cornification, which causes parakeratosis, a situation characterized by the presence of nuclei in the stratum corneum. This is responsible for the characteristic scaling. Also, the epidermis becomes greatly thickened (acanthosis), and the epidermal rete ridges are increased in length and width (papillomatosis). There is also hypogranulosis, reduction or absence of the granular cell layer, caused by the irregular and enhanced keratinocyte turnover that inhibits normal epidermal differentiation (1–4).

The precise cause of this disorder is unknown, however, some factors including the environment, genetics, immune malfunction with T cells and other white cells like neutrophils, and skin disorders such as cutting, trauma, sting, etc. are responsible. Besides, TNF alpha plays an important role in the inflammation process of psoriasis. The basic function of T cells is fight against foreign bodies like bacteria and viruses and abnormal activation of T cells ultimately triggered increased production in skin cells, also leads to production of other WBC and neutrophils which causes redness and postural lesions with pus sometimes while travelling through the skin. The area affected with psoriasis due to the dilated vessels, causes redness and warmness within the lesions of skin (5). The irregular growth of new skin cells becomes a repetitive cycle and it relocates very rapidly to the outmost layer of stratum corneum within a day instead of a week and process will never cease until treatment. The conventional treatment regimen of psoriasis results in reversal of the skin to a clinically normal state, i.e., reduction of response to the inflammatory cells and restoration of epidermal thickness. This results in many treatments being explored to achieve maximum therapeutic response. The topical therapy is the first line of treatment of psoriasis and topical corticosteroids are most commonly used for use (6).

1.2. Risk factors of Psoriasis

Psoriasis is a chronic inflammatory skin condition that is determined by a series of genetic, environmental, and behavioral components. There have been great strides in the understanding of the genetic etiology of the disease. The disease is termed a polygenic disorder, whereby several genes play a role in the progression of the disease. Certain genetic alleles like HLA-Cw6, HLA-DQ*02:01, CCHCR1, and CYP1A1 have been strongly linked with a susceptibility to developing psoriasis. In addition, various genomic locations, such as PSORS1 to PSORS9 and PSORSASI, have been found to be susceptibility loci.

Epidemiological observations in Europe have established the genetic nature of the disease. If both parents are affected, the probability of a child's developing psoriasis rises to approximately 40%. The risk decreases to around 14% when one of the parents is affected and further to 6% if only a sibling is affected. With genetic predisposition, the development and severity of psoriasis are usually determined by external factors. Environmental and lifestyle conditions like skin damage, bacterial infections, especially streptococcal infections smoking, the administration of some drugs such as lithium and interferon, and psychological stress can all worsen the condition. They can trigger or exacerbate psoriatic manifestations in genetically predisposed persons, illustrating the interplay between the environment and genes in the pathogenesis of psoriasis (6–10).

1.3 Pathology of Psoriasis

Psoriasis is an immune-mediated skin disease with a sophisticated and incompletely understood pathogenesis. One of the key mechanisms is the increased activity of elements of the adaptive immune system. During early psoriasis formation, numerous immune cells such as keratinocytes, dendritic cells, T-cells, and macrophages are stimulated by particular cytokines.

A pivotal initial event is the generation of DNA–LL37 complexes, which can trigger plasmacytoid dendritic cells to secrete interferon-alpha (IFN-α). This interferon in turn activates myeloid dendritic cells, which initiate production of interleukin-12 (IL-12) and interleukin-23 (IL-23). IL-12 is important in the differentiation of naïve T-cells to TH1 cells, whereas IL-23 drives the proliferation and survival of TH17 and TH22 cells.

These activated T-helper cells secrete a number of pro-inflammatory cytokines: IFN-γ and tumor necrosis factor-alpha (TNF-α) are secreted by TH1 cells; IL-17, IL-22, and TNF-α by TH17 cells; and

IL-22 by TH22 cells. Of these, the IL-23/TH17 pathway is thought to be especially important in psoriasis. This signaling pathway results in intracellular mediators such as Tyk2, Jak2, and STAT3 activating inflammatory gene transcription. The released cytokines are responsible for aberrant keratinocyte proliferation, enhanced angiogenesis, upregulated endothelial adhesion molecules, and recruitment of other immune cells into the skin, leading to the development of psoriatic lesions. This immune cascade is responsible for the chronic inflammation and typical characteristics of psoriasis (11–15).

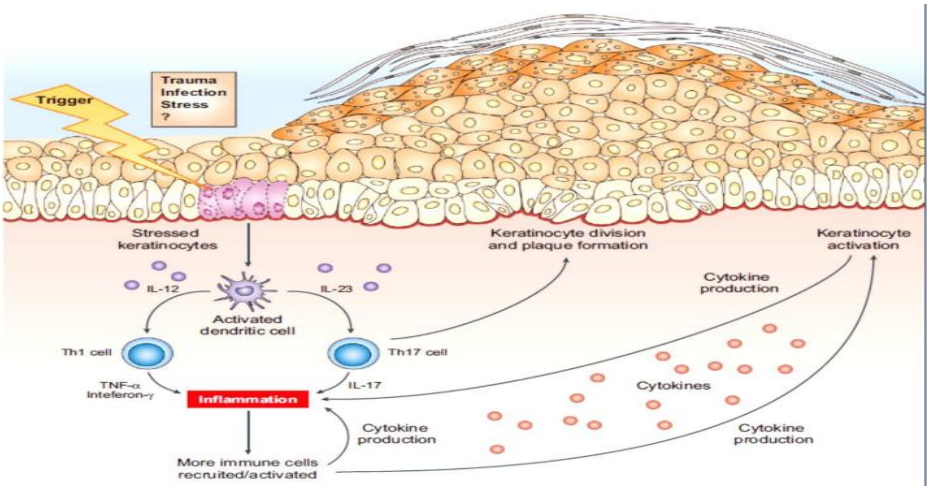

Figure 1.2: The pathophysiology of Psoriasis (Young et al., 2017)

1.4 Types of Psoriasis diseases

Skin disease

Psoriasis is a chronic autoimmune skin disease of multiple clinical presentations, with the most common being skin psoriasis. It is a papulosquamous disease with scaly, inflamed papules and plaques as characteristics. The most frequent type is psoriasis vulgaris, or plaque psoriasis, which is usually symmetrical well-defined red plaques covered with silvery-white scales. These eruptions appear generally on the scalp, elbows, knees, and lower back.

Another type, inverse psoriasis, occurs in skin creases like the armpits, groin area, under the breasts, around the navel, and between the buttocks. As opposed to plaque psoriasis, inverse psoriasis develops as smooth, glossy, red patches owing to the humid nature of these regions and is typically made worse by rubbing and sweating. Guttate psoriasis is characterized by the sudden onset of small, drop-shaped red spots, predominantly on the trunk and limbs. It is usually initiated by infections such as streptococcal throat infection and occurs more frequently in children and young adults.

Pustular psoriasis presents in the form of white pustules (blisters containing non-infectious pus) over red skin. It may be localized to the palms and soles or may be seen over large surfaces in its generalized type, which can be a medical emergency. The severe but rare type, erythrodermic psoriasis, consists of widespread redness, scaling, and peeling on large areas of the body. It can be accompanied by severe itching, pain, and body temperature changes, and can be dangerous to one's health, needing immediate medical attention. Every type of skin psoriasis is different in severity, distribution, and causes, requiring accurate diagnosis and personalized treatment (16–18).

Nail Psoriasis

Psoriatic nail disease, most commonly in the foot, tends to have characteristic clinical features of pitting—tiny, pinpoint depressions on the surface of the nail—and distal onycholysis, with the nail lifting away from the nail bed beginning at the end. These are typical signs of nail involvement in psoriatic disease.

Other significant signs are yellowish coloration (also called the "oil drop" or "salmon patch"), paronychia (paronychia or inflammation of the nail folds), subungual hyperkeratosis (thickening beneath the nail), and in advanced cases, onychodystrophy, a non-specific term for abnormal growth of the nail causing deformation or destruction of the nail plate.

Nail alterations take place in almost 50% of patients with psoriasis, expressing inflammation involving the nail matrix (the site of nail plate formation) and/or nail bed. These signs can have a major influence on quality of life, particularly if coexisting with joint or skin disease, and can be used as a clinical marker for more serious or systemic illness.

Psoriatic arthritis

Psoriatic arthritis (PsA) is an inflammatory, chronic condition that involves the joints and is observed in approximately 6–39% of patients with psoriasis, which is equivalent to around 0.1%–0.25% of the world's population. The course of PsA can be very variable, developing slowly or quickly. PsA is somewhat similar to rheumatoid arthritis (RA) in that it causes severe joint inflammation but is different in many aspects. One of the definitive characteristics of PsA is having focal erosions in the joint junctions of bones, which cause damage and deformity to joints if not treated.

1.5. Psoriasis treatment

Category	Agent	Mechanism of Action	Examples	References
Herbal	**Turmeric (Curcuma longa)**	Curcumin acts by inhibiting the activation of NF-κB, a key regulator of inflammation. This inhibition leads to a decrease in pro-inflammatory cytokines such as TNF-α, which play a major role in inflammatory processes. Additionally, curcumin helps suppress the excessive proliferation of keratinocytes, which is a characteristic feature in conditions like psoriasis.	Curcumin can be delivered through various methods to maximize its therapeutic effects. Topical formulations allow direct application to the affected skin areas, helping reduce local inflammation and keratinocyte proliferation. Nanoemulsions enhance curcumin's bioavailability and stability, improving its absorption and effectiveness when applied topically or taken orally..	(19,20)
	Neem (Azadirachta indica)	Contains nimbidin and azadirachtin, which have anti-inflammatory, immune-regulating, and wound-healing effects.	Neem oil, creams, and extracts are used for their anti-inflammatory and healing properties in skin care.	(21,22)
	Aloe Vera (Aloe barbadensis)	It contains aloin and anthraquinones, which help reduce inflammation, hydrate the skin, and speed up wound healing.	Aloe vera gels and creams contain aloin and anthraquinones that help soothe inflammation, moisturize the skin, and support faster healing.	(23–25)
	Green Tea (Camellia sinensis)	Epigallocatechin gallate (EGCG) helps by slowing down keratinocyte growth and lowering oxidative stress in the skin.	Green tea extracts and topical products contain EGCG, which helps reduce skin inflammation and controls keratinocyte overgrowth.	(26)
	Boswellia (Boswellia serrata)	Boswellic acids block 5-lipoxygenase, which lowers inflammation caused by leukotrienes.	Boswellia extracts and creams are used for their anti-inflammatory effects by inhibiting leukotriene	(27,28)

			production.	
	Guggul (Commiphora mukul)	This property is seen in compounds that reduce inflammation and oxidative stress by affecting TNF-α and IL-1 signaling pathways.	Used in both oral supplements and topical treatments.	(29,30)
	Tea Tree Oil (Melaleuca alternifolia)	Used to reduce skin irritation through its antimicrobial and anti-inflammatory effects.	Essential oils are commonly used in diluted form for topical applications to reduce skin irritation and inflammation.	(31,32)
	Licorice (Glycyrrhiza glabra)	Glycyrrhizin helps reduce inflammation by suppressing pro-inflammatory cytokines and supports skin healing and regeneration.	Used in topical creams and extracts for skin treatment.	(26,33)
Synthetic	**Corticosteroids**	These compounds reduce inflammation by blocking phospholipase A2 activity and lowering cytokine levels.	Clobetasol propionate, betamethasone, and hydrocortisone are corticosteroids used topically to reduce inflammation, itching, and redness in skin conditions like psoriasis..	(34,35)
	Vitamin D Analogues	These agents regulate keratinocyte growth and maturation by activating vitamin D receptors, helping to normalize skin cell turnover in conditions like psoriasis.	Calcipotriol and calcitriol are vitamin D analogs that help control keratinocyte proliferation and promote healthy skin cell differentiation by activating vitamin D receptors.	(36–38)

2. Nanoemulsions

Nanoemulsions are clear, stable dispersions of water, oil, and surfactant with small droplets ranging from 20 to 200 nm. These new delivery systems are better than the conventional formulations because they provide greater stability and surface area. Their small droplet size increases the solubility and bioavailability of water- and fat-soluble drugs, enabling improved drug release control. Due to the benefits listed above, nanoemulsions are incorporated into numerous pharmaceutical and cosmetic formulations and may be taken orally, applied topically, or injected (39–41).

In dermatological diseases such as psoriasis, nanoemulsions are particularly efficient since their small droplets are able to travel deep into the skin, where medication is delivered directly into affected areas. Targeted delivery enhances efficiency in treatment and minimizes side effects, positioning nanoemulsions as a promising solution for controlling dermatological diseases.

3. Importance of Nanoemulsions in Psoriasis Treatment

Psoriasis is a chronic autoimmune disorder characterized by excessive growth of skin cells, inflammation, and immune system dysregulation. Traditional topical therapies such as creams and ointments tend to find it difficult to penetrate into deeper layers of the skin, making their effectiveness limited. Nanoemulsions offer a hopeful solution through increased drug penetration, enhanced delivery directly to the site of injury, and increased overall effectiveness in psoriasis therapy. (21,42,43):

Improved Skin Penetration

The small droplet size of nanoemulsions allows them to penetrate as deep into the skin as possible, such that drugs are able to reach the desired locations effectively.

Improved Solubility and Bioavailability

Nanoemulsions enhance the solubility of poorly water-dissolvable drugs, promoting better absorption and greater treatment efficacy.

Targeted Delivery

By encapsulating drugs within small oil droplets, nanoemulsions enable delivery directly to the target area, reducing side effects in the body while increasing the treatment's potency where it is most needed.

Controlled Drug Release:

Nanoemulsions provide long-term release of active components, which provides a stable level of drug over time, maximizing therapeutic efficacy and decreasing the frequency of application.

Decreased Irritation and Improved Stability:

Nanoemulsions are not harsh on the skin because they have a mild formulation and are also long-term stable without phase separation, so they are suitable for topical application in dermatology.

Versatility of Active Ingredients:

Nanoemulsions provide a versatile platform by having both synthetic drugs like methotrexate and calcipotriol and herbal extracts like curcumin and neem oil so that a holistic and synergistic management of psoriasis becomes possible.

Enhanced Patient Compliance:

Nanoemulsion-based products such as sprays, gels, and lotions are greasy-free, spread well, and enhance comfort to the user resulting in enhanced patient satisfaction and compliance with psoriasis treatment regimens.

4. Cinnamon

The inner bark of trees in the genus Cinnamomum is where cinnamon comes from. It is a very valuable spice. Cinnamon has been used in cooking, traditional medicine, and even religious rites for hundreds of years. It has a sweet, toasty, and fragrant taste. Ceylon cinnamon (Cinnamomum verum), which is commonly called "true cinnamon," is the most well-known kind. It comes from South and Southeast Asia. Cassia cinnamon (Cinnamomum cassia) is another common kind that has a stronger, more pungent flavor.

Figure 2.1: Powder of Cinnamon

5. Review of literature

5.1 Review of literature of Cinnamon and Garlic

Table 5.1: Previously publications or patents describing different curcumin, Garlic formulations

Dosage form	Delivery route	Inference	References
Cinnamon cream	Transdermal	The Lauraceae family includes the perennial tree of tropical medicine, cinnamon (Cinnamomum zeylanicum and Cinnamomum cassia). People all across the world use cinnamon as one of the most common spices every day. Cinnamon is largely made up of essential oils and other chemicals, such cinnamaldehyde, cinnamic acid, and cinnamate. Cinnamon has several health benefits,	(44)(45)

		such as being anti-inflammatory, anti-cancer, antidiabetic, antibacterial, lipid-lowering, and lowering the risk of heart disease. It has also been shown to work against neurological illnesses including Parkinson's and Alzheimer's diseases.	
Cinnamon cream	Transdermal	The rise in germ resistance has prompted research into new antibacterial substances or methods of transmission. Escherichia coli (E. coli) is an opportunistic pathogen that forms a biofilm, leading to numerous nosocomial infections that are often difficult to eradicate with current treatments. Cinnamomum verum (cinnamon oil) is widely employed as a natural antibacterial agent, whereas solid lipid nanoparticles (SLNs) are considered promising carriers for antibacterial compounds due to their lipophilic characteristics and capacity to penetrate the bacterial cell wall effortlessly. This study entailed the formulation of nanoparticles including cinnamon oil (CO-SLN) by the dual emulsion technique, succeeded by an assessment of their particle size, shape, entrapment efficiency (EE), transmission electron microscopy (TEM), oil release kinetics, and cellular compatibility. The antibacterial effectiveness of CO-SLN and CO against 10 drug-resistant strains of E. coli was evaluated.	(46-64)

6. Methodology

6.3.1 Physical characterization and identification of Garlic and cinnamon

The obtained samples of garlic and cinnamon were examined based on their physicochemical properties, including scent, color, and solubility in both aqueous and organic solvents. We used Fourier-transform infrared spectroscopy (FTIR), ultraviolet-visible (UV-Vis) spectroscopy, and melting point analysis to check the structure and purity of the samples again. The obtained data were compared with published literature values to confirm the identity and quality of the compounds(65–67).

6.3.1.1 Organoleptic properties

The physical appearance, color, and unique smell of garlic and cinnamon were looked at as part of their first identification.

6.3.1.2 Melting point determination

Using a typical melting point apparatus and the capillary technique, we found the melting point of the sample. A little amount of the powdered medication was put into a capillary tube to make a column that was about 4 to 6 mm tall. The equipment then had a calibrated thermometer next to the capillary tube. The temperature at which the sample started to melt was noted as its melting point (68).

6.3.1.3 FTIR spectroscopy examination

We used Fourier-transform infrared (FTIR) spectroscopy to look at the functional groups in samples of garlic and cinnamon. The measurements were taken with an IR Prestige-21 spectrophotometer from Shimadzu Corp. in Japan, using the potassium bromide (KBr) pellet method. To prepare the samples, 1 mg of curcumin and 1 mg of garlic powder were each combined with an equivalent amount of dry KBr in a 1:1 ratio. To make sure the pellets were evenly distributed and formed correctly, the mixes were finely crushed and pressed into clear pellets using a hydraulic press. The FTIR spectra were taken from 4000 cm^{-1} to 400 cm^{-1}. The recorded spectra showed the functional groups that were unique to each sample. After comparing the observed spectrum patterns to conventional reference spectra, the functional groups were identified and confirmed. This made it possible to provide a qualitative assessment of the chemical makeup of both garlic and cinnamon.

6.3.1.4 Preparation of standard calibration curve by spectrophotometer technique

6.3.1.5 Standard calibration curve of Garlic and cinnamon in methanol

To examine the absorbance properties of garlic and cinnamon extract, 10 milligrams of each was accurately measured and dissolved in 10 ml of methanol to create a primary solution. Two milliliters of this stock was meticulously measured and diluted with methanol to provide a working solution with a concentration of 20 µg/ml. The conclusive volume was 100 milliliters. From this solution, many dilutions were prepared to achieve a concentration range of 1 µg/ml to 18 µg/ml. The specific concentrations prepared were 1, 2, 3, 4, and continued sequentially up to 18 µg/ml, ensuring a comprehensive range for spectrophotometric measurement. A UV-Visible spectrophotometer was employed to analyze each of these diluted samples. Absorbance measurements were conducted at two distinct wavelengths: 426 nm, the peak absorption wavelength for curcumin, and 254 nm, the typical absorption wavelength for garlic constituents. Methanol was employed as the blank to ensure the accuracy of the measurements. Following data collection, a calibration curve was constructed by plotting the mean absorbance of each sample against its concentration in µg/ml. This graph illustrates that the response is linear, consistent with Beer-Lambert's law. It may also serve as a reference for determining the concentrations of unknown substances in subsequent testing (69).

6.4 Formulation of nanoemulsion

6.4.1 Screening of excipients

Selecting the appropriate oil phase is crucial for facilitating the effective penetration of garlic and cinnamon into the skin via nanoemulsion (NE) systems. A solubility study was conducted to assess several components, including oils, surfactants, and co-surfactants. The oils studied were soybean oil, oleic acid, olive oil, black seed oil, and almond oil. Tween 80, Tween 20, Cremophor EL, and Plurololeique were evaluated as surfactants, whereas propylene glycol, PEG-400, PEG-200, and n-butanol were assessed as co-surfactants. Garlic and cinnamon were added in excess to 0.5 ml of each selected component in individual glass vials. Subsequent to an initial vortexing procedure, the vials were sealed and maintained in an upright position within a shaker incubator (Shellab, USA) at 37 ± 1 °C for 72 hours to facilitate the appropriate dissolution of the active compounds. Subsequent to incubation, the mixtures were centrifuged at 3000 rpm for 15 minutes to segregate the undissolved particles. A 0.22-µm nylon syringe filter was subsequently employed to filter the supernatants. We employed an ultra-performance liquid chromatography (UPLC) approach to assess the solubility of garlic and cinnamon in each component, as detailed in Section 2.2 of the methodology. We conducted all measurements thrice and presented the data as mean values accompanied by their standard deviations (mean ± SD) to ensure statistical validity (70–73).

6.4.2 Constriction of Pseudo Ternary Phase Diagram

Employing the aqueous titration technique, we constructed pseudoternary phase diagrams and utilized the spontaneous emulsification method to identify the nanoemulsion (NE) region. The quantity of NE points illustrated in these figures facilitated our selection of appropriate surfactant and cosurfactant combinations. Following the identification of the optimal surfactant and cosurfactant, a comprehensive analysis of the phase diagram was conducted utilizing several Smix ratios (1:1, 1:2, 1:3, 2:1, and 3:1) to determine the most effective concentration ranges for the efficient production of NE. To comprehensively analyze the behavior of the phases, each Smix ratio was evaluated with various oil-to-Smix weight ratios. There was a total of twelve unique combinations, comprising 1:8, 1:7, 1:6, 1:5, 1:4, 1:3.5, 1:3, 1:2.5, 1:1, 1:0.3, 1:52, and 1:0.3. These ratios facilitated the identification of the phase boundary, hence enabling precise delineation of the northeastern region. The aqueous phase was incrementally introduced while swirling gently for each combination. The resulting mixes were further examined to ensure the formation of transparent, low-viscosity nanoemulsions. Subsequently, Prosim software was utilized to construct the phase diagrams. Each axis represented a component of the nanoemulsion system: the aqueous phase, the oil phase, and the Smix (surfactant and cosurfactant) combination. The graphs illustrated the dimensions and configuration of the NE region at consistent mass ratios, facilitating the formulation development process by distinctly delineating the component ranges optimal for producing stable nanoemulsions (74–76).

6.4.3 Preparation of nanoemulsion formulation

Aqueous titration was utilized to create a drug-loaded nanoemulsion (NE), using oleic acid as the oil phase, Tween 80 as the surfactant, and PEG 400 as the co-surfactant, selected for their emulsification efficiency. We evaluated the solubility of the active compounds in water. Cinnamon dissolved at a rate of 0.67 µg/ml, whereas garlic dissolved at a rate ranging from 562 to 678 µg/ml. We produced an oil-in-water (O/W) nanoemulsion utilizing the spontaneous emulsification method. We used a vortex mixer (Nirmal International, Delhi, India) to amalgamate designated quantities of cinnamon and garlic into the oil phase. Subsequently, the Smix, including a blend of surfactants and co-surfactants, was incorporated into the solution. The entire mixture was vortex combined for 15 minutes and thereafter gently heated to 40 °C for 5 minutes to enhance dissolution. Distilled water was gradually incorporated into the mixture while continuously spinning. The gradual, dropwise incorporation of the aqueous phase produced a transparent, stable, and homogeneous nanoemulsion, illustrating the successful amalgamation of both bioactives inside the nanoemulsion system (77–79).

6.4.4 Thermal stability

Thermal stability tests were done to see how thermodynamically stable the produced nanoemulsions (NEs) were. The formulations were subjected to various temperature variations to assess their resistance to phase separation, changes in clarity, droplet size, and drug concentration. This evaluation was executed utilizing established approaches, with some modifications to suit the specific formulation context. In the investigation, the NEs were subjected to heat cycling and centrifugation stress to simulate storage and handling conditions. We carefully watched for signs of instability, such as turbidity, creaming, coalescence, or sedimentation. Changes in droplet size and drug concentration were also looked at to see if the physical and chemical integrity of the nanoemulsions was still intact. The test results confirmed that the formulations maintained their homogeneity and effectiveness over time under different heat settings (77).

6.4.5 Heating-Cooling Cycle

A heating-cooling cycle test was performed to assess the thermal stability of the produced nanoemulsions (NEs). The compositions saw six full temperature cycles, alternating between 4 °C and 45 °C. Each temperature setting was maintained for a minimum of 48 hours to simulate long-term storage stress and evaluate the stability of the nanoemulsions under diverse environmental conditions. At the end of all six cycles, the formulations were evaluated for signs of physical instability, including phase separation, changes in clarity, and the occurrence of precipitation or turbidity. This test was crucial for confirming the temperature stability and overall integrity of the nanoemulsion systems before proceeding to further development or storage (78).

6.4.6 Centrifugation

The nanoemulsion (NE) formulations were spun at 3,500 rpm for 30 minutes to see how stable they were under stress. This approach aimed to identify any potential for phase separation or instability at elevated centrifugal force. Formulations that stayed clear, homogeneous, and didn't show any signs of phase separation or precipitation were considered physically stable. These stable formulations were then selected for additional evaluation using the freeze-thaw method to test their durability against extreme temperature fluctuations (79).

6.4.7 Freeze-Thaw cycle

We did freeze-thaw tests on the stable nanoemulsion (NE) formulations after centrifugation to see how stable they were at high temperatures. The formulations went through three freeze-thaw cycles, with storage conditions changing from -21 °C to +25 °C. To simulate hard storage conditions, each temperature setting was held for at least 48 hours per cycle. This test was set up to see if the formulations could handle heat stress without breaking down, forming crystals, or changing their look. Formulations that stayed clear, even,, and stable after freeze-thaw cycles were considered thermodynamically stable and ready for further development (80).

6.5 Evaluation of nanoemulsion

6.5.1 Globule size and Polydispersity Index analysis

About 50 µl of the nanoemulsion (NE) formulation was taken out and mixed with 2 ml of distilled water to get the right amount of scattering for analysis. A Zetasizer Nano-ZS90 (Malvern Instruments, Worcestershire, UK) was used to look at the size of the globules and the polydispersity index (PDI) of the diluted sample. This machine uses dynamic light scattering (DLS) to find out how big the particles are and how evenly they are

spread out in the formulation. To ensure accuracy and consistency, measurements were taken three times, and the average droplet size was calculated from these measurements. This study provided insights into the stability of size and the homogeneity of dispersion of the produced nanoemulsions (81).

6.5.2 Transmission electron microscopy (TEM)

We used a Philips CM 200 transmission electron microscope to look at the shape of the scattered oil globules in the nanoemulsion. The microscope is from Briarcliff Manor, NY, USA. To prepare the sample, the NE formulation was first mixed with distilled water in a 1:900 ratio to get the best particle dispersion. A small amount of the diluted sample was carefully placed on a copper grid that had been coated with carbon. To make the image stand out more, negative staining was done on the grid with 2% w/v phosphotungstic acid. Before being analyzed, the stained specimen was allowed to air dry for one minute. The TEM imaging gave a full view of the nanoemulsion's globule structure, confirming that the oil droplets were evenly spread out and had a spherical shape (82).

6.5.3 Viscosity and reflective index

We used Abbe's refractometer (Precision Standard Testing Equipment Corp., Germany) to measure the refractive index of the nanoemulsion (NE) formulation. This gave us information about how clear and even the system is. A Brookfield viscometer (MCR101, Rheoplus, Anton Paar India Pvt. Ltd.) was used to measure viscosity in order to see how the formulations flowed and how consistent they were. This study clarified the rheological characteristics of the NE, which are crucial for predicting its stability, application efficiency, and overall effectiveness in topical or alternate administration techniques (83).

6.5.4 pH and Transmittance

We used a calibrated pH meter (Mettler Toledo, Langacher, Switzerland) to check the pH of the nanoemulsion at 25 °C to make sure it was compatible with physiological conditions, following the approach described by Mahtab et al. (2016). Along with checking the pH, transmittance analysis was used to check how clear the formulation was. We put one milliliter of the nanoemulsion into a clean cuvette and used a UV-Vis spectrophotometer (UV 1601, Shimadzu, Japan) to measure it three times at a wavelength of 630 nanometers. High transmittance values meant that a clear and stable nanoemulsion had been made, which proved that the oil droplets were evenly spread throughout the water phase (84,85).

6.5.5 Skin irritation study

A comparative study on skin irritation was conducted on albino rats using the Draize scoring method to evaluate the irritation potential of the nanoemulsion (NE) formulation in comparison to a standard irritant, a 0.8% v/v formalin solution. The rats were divided into two groups: a healthy control group that did not get any treatment and a group that did get the NE formulation. At regular intervals, the treated skin areas were checked for signs of discomfort, such as redness and swelling. A nearby region of skin that wasn't treated served as the control for comparison. Using the Draize scale, we visually examined the treated and control areas and gave them ratings that showed how irritated they were. The Primary Irritation Score (PIS) was calculated for each area, and the difference between the total PIS for the treated and untreated locations was used to find the Primary Irritation Index (PII). This metric made it possible to compare the irritation caused by the NE formulation to untreated skin (86,87).

6.5.6 Skin Permeation

The membrane model for the ex vivo permeation studies was made from rat skin taken from the abdomen. Before the excision, a depilatory cream was used to carefully remove hair from the dorsal area to avoid interfering with the follicles. After the excision, the subcutaneous adipose tissue was carefully taken off the dermal side using surgical dissection. Then, isopropyl alcohol was used to clean it up and make it smooth and even. The excised skin was equilibrated in a 0.9% sodium chloride solution for 30 minutes to maintain its physiological integrity before being put on Franz diffusion cells. The Franz diffusion apparatus used had an effective diffusion area of 0.80 cm^2 and a receptor chamber that could hold 11 ml. To guarantee sink conditions, the solubility of the test medications was assessed in a combination of phosphate buffer (pH 7.4) and isopropyl alcohol at an 8:2 (v/v) ratio, which was also utilized to fill the receptor chamber. A magnetic stirrer running at 100 rpm kept the complete assembly at 37 ± 1 °C, which is how it would be in a live body. In the experiment, 1 ml of the nanoemulsion (NE) was placed in the donor chamber, which was then sealed with paraffin film to keep the conditions

from getting too wet. At predetermined time points (0.25, 0.5, 1, 2, 4, 6, 8, 12, and 24 hours), 1 ml samples were withdrawn from the receptor compartment and immediately replaced with fresh phosphate buffer solution to maintain volume and sink conditions. The collected samples were filtered through a 0.45 µm membrane filter and then tested for drug content using a method that had already been described. This arrangement made it possible to accurately measure how well drugs passed through the skin during a 24-hour period. For the ex vivo permeation investigations, rat skin taken from the abdomen was employed as the model for the membrane. Prior to excision, hair was carefully removed from the dorsal surface using a depilatory cream to avoid follicular interference. After the excision, surgical dissection carefully removed subcutaneous fat from the dermal side. Then, isopropyl alcohol was used to polish the surface even further to make sure it was smooth and even. The excised skin was equilibrated in a 0.9% sodium chloride solution for 30 minutes to preserve its physiological integrity before being affixed to Franz diffusion cells. The Franz diffusion apparatus used had an effective diffusion area of 0.80 cm^2 and a receptor chamber volume of 11 ml. To ensure sink conditions, the solubility of the test drugs was determined in a mixture of phosphate buffer (pH 7.4) and isopropyl alcohol in an 8:2 (v/v) ratio, which was also used to fill the receptor chamber. The entire assembly was maintained at 37 ± 1 °C using a magnetic stirrer set at 100 rpm to mimic in vivo conditions. For the experiment, 1 ml of the nanoemulsion (NE) was placed into the donor chamber, which was then sealed with paraffin film to maintain occlusive conditions. At predetermined time points (0.25, 0.5, 1, 2, 4, 6, 8, 12, and 24 hours), 1 ml samples were withdrawn from the receptor compartment and immediately replaced with fresh phosphate buffer solution to maintain volume and sink conditions. The collected samples were filtered through a 0.45 µm membrane filter and analyzed for drug content using a validated analytical method described previously. This setup allowed for the accurate assessment of drug permeation through the skin over a 24-hour period (88,89).

6.5.7 Stability study

We prepared three batches of the better nanoemulsion (NE) formulations and put them in glass vials to see how stable they were. The samples were kept in controlled environmental settings according to the International Conference on Harmonization (ICH) criteria. One set was kept at 25 °C ± 2 °C and 60% ± 5% relative humidity (RH), and the other set was kept at 40 °C ± 2 °C and 75% ± 5% RH. For more than three months, important physical characteristics such droplet size, polydispersity index (PDI), viscosity, refractive index, pH, and transmittance were carefully looked at to see if the formulation changed. For these trials, samples were taken at set times: 0, 1, 2, and 3 months. We looked at the formulations' appearance and clarity at the beginning and after 30 days to see whether there were any signs of instability, such as turbidity, precipitation, or phase separation. This rigorous test showed that the nanoemulsion kept its intended properties and stability during the storage period (90–92).

6.5.8 Statistical analysis

Prosim software was used to do the statistical analysis. We used a two-way analysis of variance (ANOVA) to look at the data, and then the Bonferroni post hoc test to compare the results. All tests were conducted in triplicate to ensure repeatability, and results are presented as mean ± standard deviation (SD). A p-value less than 0.05 was considered statistically significant, indicating considerable differences across the examined groups.

RESULTS AND DISCUSSION

7.1 Results

7.1.1 Preformulation Studies

7.1.1.1 Physical and characterization and identification of Garlic and cinnamon

Table 7.1: Physical and characterization and identification of Garlic and cinnamon

S. No.	Parameters	Inferences	
		Garlic	cinnamon
1	Nature	Powder	Amorphous powder
2	Colour	off-white	Reddish-brown
3	Order	Strong, pungen	Sweet, warm, and aromatic fragrance
4	Taste	Spicy, and slightly hot with	Sweet, warm, and slightly woody

		a lingering pungency.	

7.1.1.2 Melting point

Using the capillary method, the melting points of garlic and cinnamon were determined to be 165°C and −7°C, respectively. These values closely match the reported melting points of 165°C for garlic and −7°C for cinnamon.

7.1.1.3 FTIR

FTIR spectra shows characteristic peaks of drug garlic and cinnamon mentioned in the Table 7.2 and 7.3 almost matched when compared with standard reference as shown in the Figure 7.1 and 7.2.

Table 7.2: FTIR Observation table of Garlic

S. No.	Observed pealk of sample (cm^{-1})	Name of group
1	3266	O-H Stretching
2	2926	C-H Stretching
3	1916	C=O Stretching
4	1395	O-H Stretching
5	1036	S=O Stretching

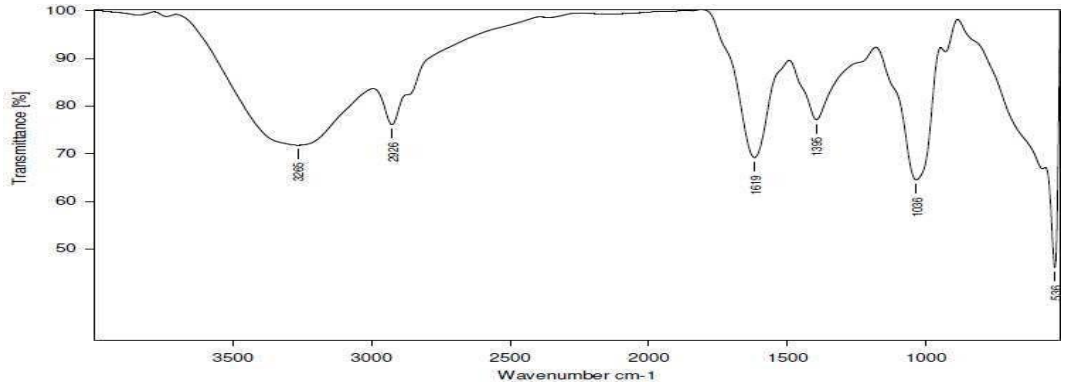

Figure 7.1: FTIR of Garlic

7.1.1.4 FTIR of Cinnamon

Table 7.3: FTIR Observation table of cinnamon

S. No.	Observed pealk of sample (cm^{-1})	Name of group
1	3008.76	C=C Stretching
2	2924.97	C-H Stretching
3	2854.42	C=O Stretching
4	1463.87	O-H Stretching
5	1163.36	C-H Stretching

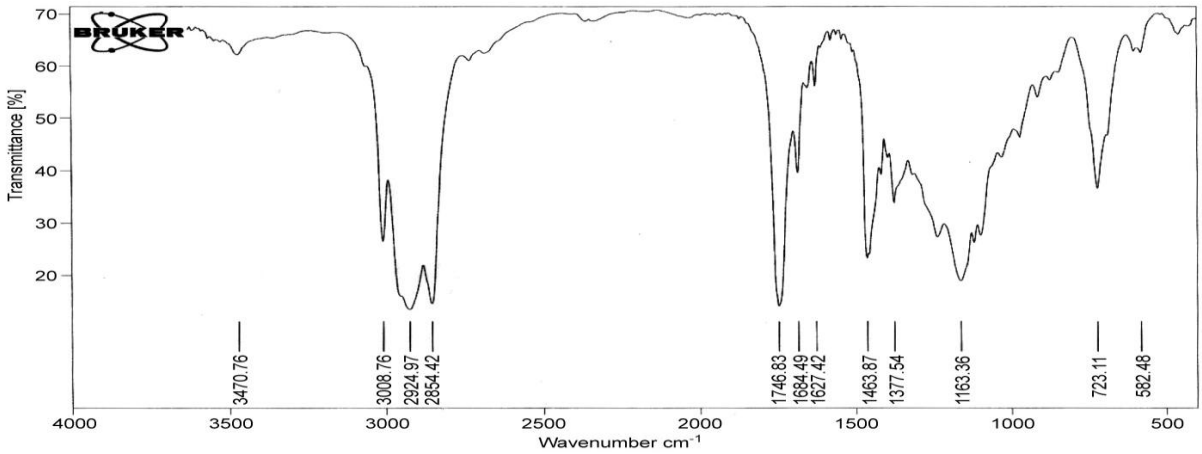

Figure 7.2: FTIR of Cinnamon

International Journal of Pharmaceutical Drug Design (IJPDD)
Website: https://ijpdd.org/
ISSN: 2584-2897
Vol. 2, Issue 12, December, 2025
Page No.: 01-25

7.1.1.5 Preparation of standard calibration curve with spectrophotometer

7.1.1.6 Calibration curve of Garlic and cinnamon in methanol

The calibration curves for garlic and cinnamon extracts in methanol were created using the right approach, and the findings are shown in the figure that goes with them. The regression coefficient (R^2) values for all medicines in both methanol and phosphate buffer solutions exhibited strong linearity within the designated concentration ranges. This shows that UV spectral analysis is a reliable way to measure these drugs. The table shows the linear equations and R^2 values for each drug in the right solvents.

7.1.1.6.1 Calibration curve of Garlic

Table 7.4: Observation table of Calibration curve of Garlic

S. No.	Concentration (µg/ml)	Absorbance	R^2
1	2	0.5120	0.998
2	4	1.1421	
3	6	0.2341	
4	8	0.3215	
5	10	0.4764	
6	12	0.5342	

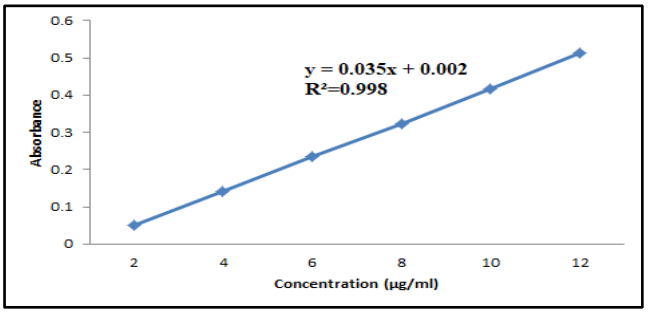

Figure 7.3: Standard calibration curve of Garlic

7.1.1.6.2 Calibration curve of cinnamon

Table 7.5: Observation table of Calibration curve of cinnamon

S. No.	Concentration (µg/ml)	Absorbance	R^2
1	2	0.0412	0.997
2	4	0.1322	
3	6	0.2143	
4	8	0.3116	
5	10	0.4165	
6	12	0.5141	

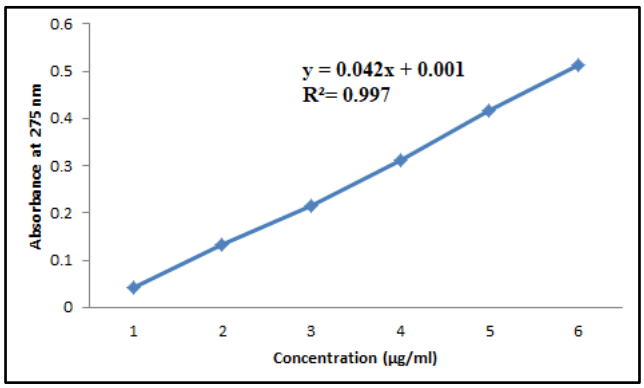

Figure 7.4: Standard calibration curve of Garlic

7.1.2 Formulation of nanoemulsion

7.1.2.1 Screening of excipients

To dissolve all the two drugs Garlic and cinnamon in a single solvent, screenings were performed as only the solubilized drug can cross the dermal layer. The solubility of all the three drugs was performed in various oils, surfactants, and co-surfactants to select the appropriate solvents for the preparation of NEs. All excipients selected for the formulation come under the "Generally-Recognized-as-Safe" (GRAS) category and are non-irritant to the skin and pharmaceutically active. For the NE formulation, maintenance of drugs in the solubilized form was required, so for this, drug solubility in oil is very essential. The results for the solubility of Garlic and cinnamon were determined in different oils, surfactants and co-surfactants were shown in Table 7.6. Amongst the various experimental oils, highest solubility (mg/ml) of Garlic and cinnamon (320.29 ± 0.40, 26.12 ± 0.62 and 8.72 ± 0.06) was observed in oleic acid and as per the earlier studies, oleic acid has a permeation enhancing characteristic, hence opted as an oil phase. Tween 80 and PEG 400 were selected as the surfactant and co-surfactant, respectively, since they indicated maximum drug solubility for Garlic and cinnamon i.e. 109.43 ± 03.68, 3.45 ± 0.75, 12.20 ± 01.29 mg/ml and 110.145 ± 03.21, 80.1 ± 02.15, 180.1 ± 05.28mg/ml, respectively. For o/w emulsion, HLB should be greater than 10 for surfactant, and HLB value for Tween 20 is 16.7

Table 7.6: Results of screening of excipients

Name of excipients	**Drug (mg/ml)**	
Oils	**Cinnamon**	**Garlic**
Oleic acid	322.30 ±0.30	28.98 ±0.76
Olive oil	16.21 ±0.12	14.09 ±0.32
Castor oil	21.25 ±0.56	7.98 ±0.34
Surfactant		
Tween 80	108.34±0.65	16.09±0.98
Tween 20	70.87±0.72	12.97±0.67
Cosurfactants		
PEG 400	109.09±0.78	120.90±0.87
PEG 200	42.98±0.27	160.98±0.56

7.1.2.2 Construction Pseudo Ternary Phase diagram

Pseudo ternary phase diagrams were prepared with 1:1, 1:2, 1:3, 2:1, 3:1, weight ratios of Smix (Tween 80:PEG400), as shown in Figure 5.17. Phase diagrams were plots using oleic acid as an oil phase, Tween 80 as surfactant and PEG 400 as cosurfactant. A small or large nanoemulsion area depends primarily upon the capacity of the individual Smix to solubilize the oil phase and also on its nanoemulsion formulation. The nanoemulsion area was found very less after using of Tween 80 alone, suggesting the fact that need of cosurfactant is required for the formation of NE formulations to achieve the flexible interfacial film with reduced negative interfacial tension. After using Tween 80 with PEG 400 (Smix ratio 1:1), a significant increase was observed in NE region as discussed above, the use of PEG 400 as a co-surfactant, reduces the bending stress of the interface, as required in NE formulation. From the Figure, decreased NE area was observed, by increasing the concentration of the cosurfactant ratio in contrast to Tween 20, which reduces the solubilization potential of NE because of reduction in micelles formation. On the other hand, when the concentration of PEG 200 was decreased with respect to Tween 20, NE area was increased. It was also noticed from 7.6 that increase in Tween 80 as compared to constant PEG 400 concentration there was no increment in the NE area. In short, the system developed a large isotropic NE area at Smix ratio 2:1 relative to the systems at other Smix ratios because of its ability to further solubilize the oil phase and to reduce the free energy system and to produce further emulsification,. Hence Smix ratio 2:1 showed maximum area which was determined by cut and weigh method and was selected for NE formulation.

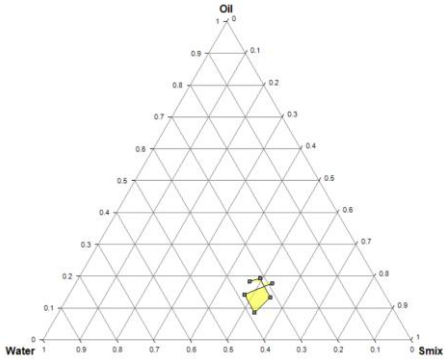

Figure 7.5: Pseudo ternary phase diagram of nanoemulsion with Smix ratio (1:1)

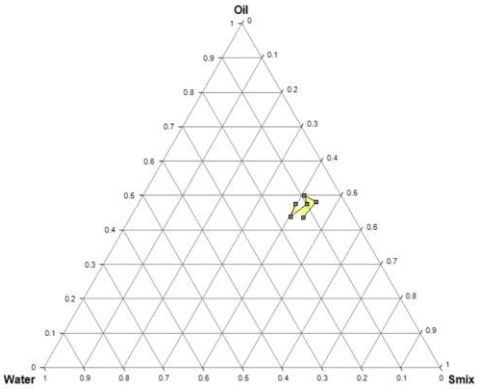

Figure 7.6: Pseudo ternary phase diagram of nanoemulsion with Smix ratio (1:2)

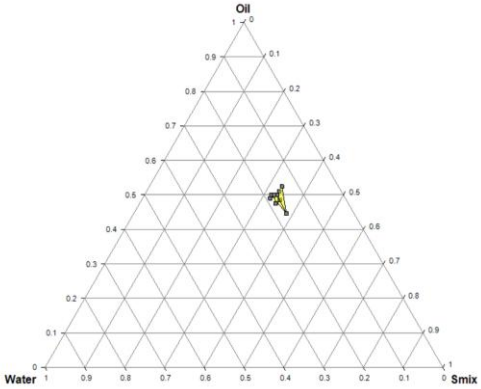

Figure 7.7: Pseudo ternary phase diagram of nanoemulsion with Smix ratio (1:3)

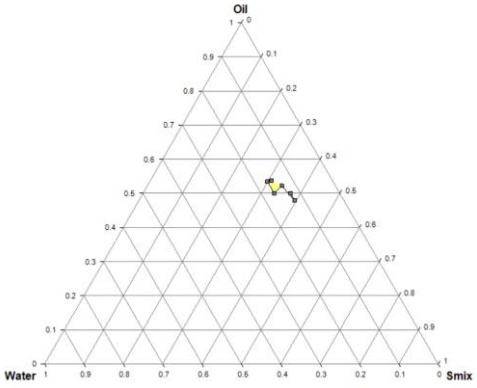

Figure 7.8: Pseudo ternary phase diagram of nanoemulsion with Smix ratio (3:1)

International Journal of Pharmaceutical Drug Design (IJPDD)
Website: https://ijpdd.org/
ISSN: 2584-2897
Vol. 2, Issue 12, December, 2025
Page No.: 01-25

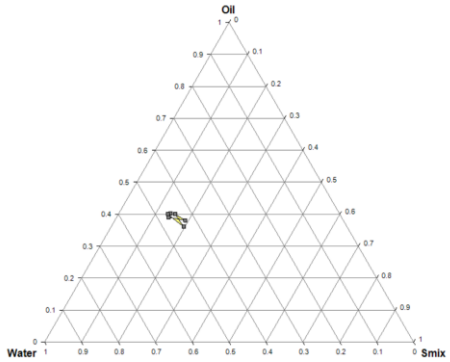

Figure 7.9: Pseudo ternary phase diagram of nanoemulsion with Smix ratio (2:1)

7.1.2.3 Preparation of Nanoemulsion Formulation

Nanoemulsions were formulated using the aqueous titration method, aiming to improve drug delivery to the dermal layers through topical application. To minimize potential skin irritation, the formulation required a careful balance of surfactant and co-surfactant. Tween 80, a non-ionic surfactant, was selected due to its lower toxicity and stability across different pH levels and ionic strengths. Polyethylene glycol 400 (PEG-400) was used as the co-surfactant, aiding in lowering interfacial tension and enhancing the flexibility of the emulsion interface, thereby promoting efficient drug diffusion. To reduce skin irritation risks associated with high surfactant levels, formulations with Smix ratios of 3:1 and 1:3 were excluded. Based on the nanoemulsion region identified in the phase diagram, three Smix ratios 1:1, 1:2, and 2:1 were selected for further development and evaluation.

Table 7.7: Composition of nanoemulsion and their thermodynamic stability

Smix ratio	Formulation code	Percentage of component			Total Volume	Observation			Results
		Oil	Smix	Water		HC	FT	Cent	
1:1 (A)	A1	3.5	24.5	82	110	P	F	P	Passed
	A2	4	19	87	110	P	P	P	Passed
	A3	2.5	21.5	86	110	P	F	F	Fail
	A4	5	22	83	110	P	P	F	Passed
1:2 (B)	B1	4	20	86	110	F	P	P	Fail
	B2	5	22	83	110	F	P	F	Fail
	B3	3	18	89	110	P	P	F	Passed
	B4	4	22	84	110	F	F	F	Fail
2:1(C)	C1	4.5	20.5	85	110	F	F	P	Fail
	C2	2.5	23.5	84	110	P	F	F	fail
	C3	5	25	80	110	F	F	F	Fail
	C4	3	29	78	110	P	P	F	Passed

7.1.2.3.1 Thermodynamic Stability and Selection of Nanoemulsion Formulations

Unlike nanoemulsions are kinetically stable but not thermodynamically stable. They are formed by optimizing specific ratios of oil, Smix (surfactant and co-surfactant mixture), and water without signs of creaming, cracking, or phase separation. The prepared formulations were subjected to thermodynamic stability tests, including heating-cooling cycles, centrifugation, and freeze-thaw procedures. Some formulations became turbid or showed phase separation during these tests, as detailed in Table 7.7. The observed instability was attributed to Ostwald ripening—a process where smaller droplets dissolve and redeposit onto larger ones, driven by surface energy gradients. Only the formulations that remained stable without phase separation were selected for further analysis.

7.1.2.3.2 Drug Loading and Optimization of Nanoemulsion Formulation

Formulations that passed initial physical stability screening were selected for drug loading. Garlic

International Journal of Pharmaceutical Drug Design (IJPDD)
Website: https://ijpdd.org/
ISSN: 2584-2897
Vol. 2, Issue 12, December, 2025
Page No.: 01-25

and cinnamon extracts, each at a concentration of 3 mg/mL, were dissolved in the oil phase. Distilled water was then added gradually until a clear, transparent nanoemulsion was formed. All drug-loaded formulations were subjected to further physical stability tests. Among them, formulation A2 demonstrated superior stability and consistent characterization results, as summarized in the table. Therefore, A2 was identified as the optimized formulation for subsequent studies.

7.1.3 Evaluation parameters of optimized formulation A2 of nanoemulsion

7.1.3.1 Globule size and polydispersity index examination

NE was found transparent and monophasic which have a droplet size of 50.00±1.57 nm, and uniform PDI of 0.14±0.03. However, as shown in Table 7.8. PDI values, a measure of droplet size uniformity within the formulation, have also been determined. There was a narrow size distribution of all the NE formulations (PDI 0.14-0.26) was found, due to a higher concentration of surfactant formed closely packed film at the interface of oil-water, provided greater stabilization, suggested that surfactant has significant function than cosurfactant, for the emulsification of oily mixture. Therefore, the size distribution of globules and consistency of the formulation is higher when there is a lesser PDI.

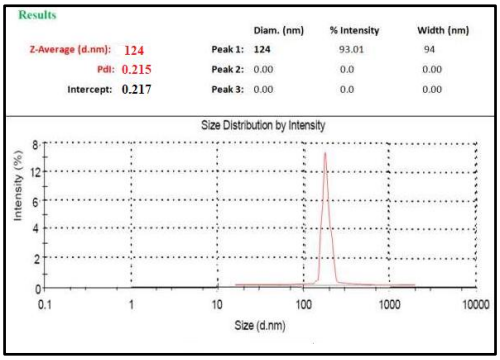

Figure 7.10: Globule size distribution of optimized nanoemulsion formulation

7.1.3.2 Transmission electron microscopy (TEM)

It is evident from the figure that the optimized nanoemulsion (NE) exhibited no visible aggregates, indicating a uniform and homogenous distribution of spherical globules throughout the formulation. These visual observations are consistent with the droplet size analysis obtained using the Zetasizer, confirming the stability and nanoscale uniformity of the formulation.

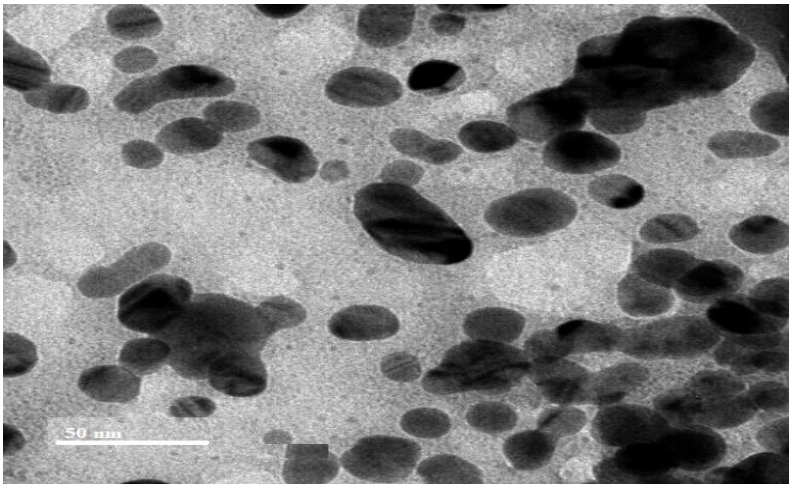

Figure 7.11: TEM of optimized nanoemulsion formulation

7.1.3.3 Viscosity and refractive index

As shown in table 7.8, the mean refractive index (RI) values for drug-loaded nanoemulsion (NE) formulations were almost the same. This shows that the system is isotropic and chemically stable. The improved formulation has a viscosity of 140.8 ± 3.027 cp and a RI of 1.405 ± 0.006. Formulations with drugs in them had a viscosity that was rather low, which is what you would expect from oil-in-water (o/w) emulsions. The low viscosity is owing to the low oil content and the usage of Tween 80, a

surfactant that has a high inherent viscosity since it is made up of polyhydric alcohol and fatty acid.

7.1.3.4 pH and transmittance

The optimized nanoemulsion formulation had a pH of 6.5 ± 0.52 and a transmittance value of 97.56 ± 0.06%, which means that the formulation was stable. As indicated in table 7.8, the pH range of drug-loaded nanoemulsions was between 6.5 and 6.8, which is good for putting on the skin. The medicine did not have a big effect on the pH. The high and steady transmittance values show that the oil globules are evenly spread out throughout the continuous phase. Also, most of the oil droplets were less than one-fourth the wavelength of visible light, which made the nanoemulsion look clear.

Table 7.8: Physical characterization study of different nanoemulsion formulation (Mean ± SD, n=3)

Formulation code	Evaluation parameters				
	Size (nm)	PDI	pH	RI	Viscosity (cP)
A1	326.5±1.76	0.22±0.06	6.8±0.66	1.534±0.003	60.5±3.76
A2	50.00±1.57	0.14±0.03	6.5±0.52	1.405±0.006	140.8±3.02
A4	178.4±1.24	0.26±0.05	6.7±0.15	1.392±0.004	84.8±4.87
B3	120.6±1.52	0.18±0.09	6.8±0.65	1.410±0.002	142.9±3.87
B4	158.6±1.56	0.21±0.87	6.6±0.17	1.364±0.008	160.8±4.26

7.1.3.5 Ex Vivo Skin Permeation Study

The ex vivo skin permeation study employed freshly excised porcine ear skin obtained from a local butcher. Pig skin closely resembles human skin in structure, with a stratum corneum (SC) thickness of 21–26 µm and an average of 20 hair follicles per cm², comparable to human forehead skin, which has 14–32 hair follicles per cm². Pig ear skin is considered a suitable model for topical drug delivery study due to its similarity, accessibility, and extensive use in permeation studies.

A stationary Franz diffusion cell with a cross-sectional area of 3.14 cm² and a receptor volume of 30 mL was used to attach the depilated dorsal skin. The stratum corneum faced the donor compartment, and the dermis touched the receptor fluid. Several formulations including 1.5 mg of garlic and cinnamon nanoemulsions were introduced into the donor chamber. Permeation profiles were defined and compared with a typical carbopol gel (CG). We calculated important numbers including permeation flow, permeability coefficient, enhancement ratio, and skin deposition. Formulation A2 had a far better penetration than the unmodified carbopol gel, with enhancement ratios of 2.934 for Garlic and 2.741 for Cinnamon. A2's permeation flow was 8.93 ± 0.97 µg/cm²/h, which was much higher than CG's 2.68 ± 0.87 µg/cm²/h ($p < 0.01$). This enhancement is attributed to polymeric micelles that alter the lipids in the stratum corneum, acting as penetration enhancers. Also, because micelles are so small, they have a larger surface area that comes into touch with the skin, which helps them get absorbed mostly by transappendageal channels, such hair follicles.

Compared to regular gels, the hydrogel formulations had a higher rate of penetration into the skin. The nanoemulgel's outstanding penetration effectiveness (8.93 ± 0.97 µg/cm²/h) emphasizes its merits, considering the apparent formulation issues connected to the integration of nanoemulsions into carbomer-based gels.

Table 7.9: Permeation flux and skin deposition of hyderogel after 24 hours.

Formulation code	Permeation Flux Jss (µg cm^{-2} h^{-1})	Permeation coefficient, Kp (cm h^{-1}) (10^3)	Enhancement ratio, Er	Skin retention (%)
A1	8.45±0.65	4.99	2.876	52.97±1.76
A2	8.93±0.97	4.66	2.653	43.52±1.37
A4	8.68±0.74	5.18	3.124	45.87±1.38
B3	8.23±0.35	4.85	2.364	48.98±1.49
B4	8.12±0.26	4.78	3.872	44.94±1.23
CG	2.68±0.87	1.88	-	8.09±2.98

International Journal of Pharmaceutical Drug Design (IJPDD)
Website: https://ijpdd.org/
ISSN: 2584-2897
Vol. 2, Issue 12, December, 2025
Page No.: 01-25

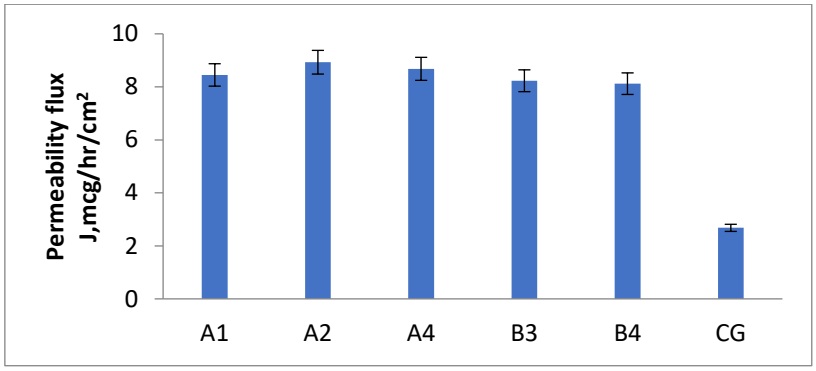

Figure 7.12: Permeability flux of different hydrogel formulation

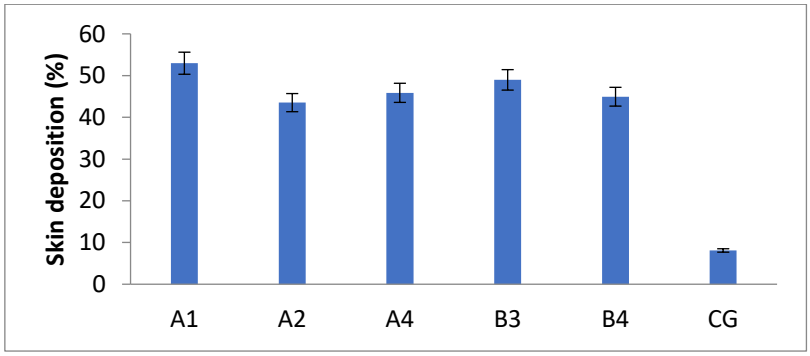

Figure 7.13: Skin deposition (%) of different hydrogel formulation

7.1.3.6 Stability study

Stability Studies as per ICH Guidelines: Physical Stability of Nanoemulsion

According to ICH recommendations, it is necessary to thoroughly assess a drug product's physical, chemical, and microbiological stability from the commencement of the research and during its designated shelf life. For nanoemulsions, physical stability is an important quality trait that can be measured by looking at things like droplet size, polydispersity index (PDI), viscosity, refractive index, pH, and transmittance.

The improved nanoemulsion formulation was kept at 25°C and 40°C for 1, 2, and 3 months in a stability study. It was seen that the size of the droplets grew a little bit over time at 25°C. At 40°C, however, a more significant increase in droplet size was observed, rising from 50.00 ± 1.57 nm to 67.14 ± 1.75 nm, mostly owing to Ostwald ripening. Other metrics showed small changes in both situations.

One-way ANOVA and the Tukey-Kramer test (GraphPad Instat) demonstrated that there were no significant changes ($P \geq 0.05$), which means that the formulation stayed physically stable over the testing period. These results indicate that the nanoemulsion maintains stability under rapid and prolonged storage settings.

Table 7.10: Stability study of optimized nanoemulsion formulation with 3 mounts

Condition	Time (Days)	Mean drop size (nm) ± SD	PDI±SD	pH±SD	RI±SD	V (cP) ±SD	Transmittace (%)±SD
25^0C±2^0C/60%±5 %	0	50.00±1.57	0.14±0.03	6.5±0.52	1.405±0.006	140.8±3.02	97.56 ± 0.06
	30	54.98±1.7	0.16±0.04	6.6±0.56	1.421±0.007	142.7±2.05	96.98±0.07
	60	62.89±2.8	0.18±0.06	6.6±0.57	1.455±0.005	144.8±1.67	96.87±0.06
	90	64.81±1.8	0.21±0.54	6.6±0.002	1.541±0.004	145.21.98	96.45±0.05

$40^0C \pm 2^0C$/75%±5 %	0	50.00±1.57	0.14±0.03	6.5±0.52	1.405±0.006	140.8±3.02	97.56 ± 0.06
	30	62.87±1.45	0.17±0.05	6.6±0.56	1.420±0.007	152.9±2.65	96.68±0.08
	60	65.98±1.76	0.21±0.07	6.6±0.74	1.453±0.006	162±1.27	95.98±0.09
	90	67.14±1.75	0.28±0.003	6.7±0.09	1.527±0.005	168±2.98	95.02±0.08

7.2 Discussion

The preformulation studies found that garlic and cinnamon have distinct physical and chemical characteristics that are important for developing formulations. Garlic looked like a white powder that smelled bad, whereas cinnamon looked like a reddish-brown amorphous material that smelled good. The melting points of garlic (165°C) and cinnamon (-7°C) matched what was already known about them, which confirmed their identity and purity. The FTIR spectra confirmed the presence of functional groups associated with each molecule, hence validating their structural attributes.

The UV spectrophotometric calibration curves showed very good linearity (R^2 ~0.998 for garlic and ~0.997 for cinnamon), which showed that they were good for quantitative analysis in methanol. These results provide a solid foundation for creating successful nanoemulsions. They make sure that both active ingredients are chemically stable, easy to identify, and easy to measure in a lab.

The nanoemulsion (NE) formulations were developed using aqueous titration employing oleic acid, Tween 80, and PEG 400, selected based on solubility screening results. The phase diagrams showed that Smix 2:1 created the biggest NE zone, which made emulsification easier. A2 (Smix 1:1) was found to be the best formulation out of all the ones tested since it was thermodynamically stable, had little phase separation, and had the right physical qualities.

Formulation A2 had better physicochemical properties for topical use, such as a very small droplet size (50.00 ± 1.57 nm), a low polydispersity index (0.14 ± 0.03), and a good pH (6.5 ± 0.52). A high transmittance (97.56%) and spherical globules seen with TEM revealed that the particles were evenly spread out and uniform on a nanoscale. The viscosity (140.8 ± 3.02 cp) and refractive index (1.405 ± 0.006) were both suitable for topical use, which means they spread well and are isotropic.

Ex vivo permeation studies using pig skin showed that A2 had a much higher flow than the conventional gel. The enhancement ratios for garlic and cinnamon were 2.934 and 2.741, respectively. The small size of the droplets and the breakdown of the stratum corneum by surfactants made transappendageal absorption possible.

Stability tests done according to ICH standards showed that there were very few changes over the course of three months. A2 stayed physically stable under both normal and sped-up conditions, even if the size of the droplets did get a bit bigger.

Conclusion

This study successfully characterized the physical and chemical properties of garlic and cinnamon by thorough inquiry, including organoleptic evaluation, melting point determination, and FTIR spectrum analysis. These parameters confirmed the identity and purity of both phytoconstituents. The UV-spectrophotometric calibration curves provided additional validation of their quantification, demonstrating substantial linearity.

We made a stable nanoemulsion by mixing garlic and cinnamon with oleic acid as the oil phase, Tween 80 as the surfactant, and PEG 400 as the co-surfactant. The pseudo-ternary phase diagrams made it easier to find the best Smix ratios. The 2:1 ratio had the biggest nanoemulsion zone. The droplet size, PDI, pH, viscosity, refractive index, and transmittance values of the produced formulations all showed that A2 was the most promising. This was because they all showed very good physical stability. Transmission electron microscopy (TEM) confirmed a uniform and spherical globule morphology, while ex vivo skin permeation assays demonstrated significantly enhanced penetration and retention of the active compounds compared to conventional gels. The formulation passed thermodynamic and accelerated stability tests, which is what ICH says it should do.

References

1. de Carvalho AVE, Leite LL. Psoriasis. In: Dermatology in Public Health

Environments: A Comprehensive Textbook, Second Edition. 2023.
2. Raharja A, Mahil SK, Barker JN. Psoriasis: A brief overview. Clinical Medicine, Journal of the Royal College of Physicians of London. 2021.
3. Canal-García E, Bosch-Amate X, Belinchón I, Puig L. Nail Psoriasis. Actas Dermo-Sifiliograficas. 2022.
4. Yamazaki F. Psoriasis: Comorbidities. Journal of Dermatology. 2021.
5. Engler D, Chezuba HP, Masuku P. Psoriasis. SA Pharmaceutical Journal. 2017.
6. Dand N, Mahil SK, Capon F, Smith CH, Simpson MA, Barker JN. Psoriasis and genetics. Acta Dermato-Venereologica. 2020.
7. Kamiya K, Kishimoto M, Sugai J, Komine M, Ohtsuki M. Risk factors for the development of psoriasis. International Journal of Molecular Sciences. 2019.
8. Kanda N, Hoashi T, Saeki H. Nutrition and psoriasis. International Journal of Molecular Sciences. 2020.
9. Garbicz J, Całyniuk B, Górski M, Buczkowska M, Piecuch M, Kulik A, et al. Nutritional therapy in persons suffering from psoriasis. Nutrients. 2022.
10. Zhou S, Yao Z. Roles of Infection in Psoriasis. International Journal of Molecular Sciences. 2022.
11. Guo J, Zhang H, Lin W, Lu L, Su J, Chen X. Signaling pathways and targeted therapies for psoriasis. Signal Transduction and Targeted Therapy. 2023.
12. Zhang X, Shi L, Sun T, Guo K, Geng S. Dysbiosis of gut microbiota and its correlation with dysregulation of cytokines in psoriasis patients. BMC Microbiol. 2021;
13. Neu SD, Strzepa A, Martin D, Sorci-Thomas MG, Pritchard KA, Dittel BN. Myeloperoxidase inhibition ameliorates plaque psoriasis in mice. Antioxidants. 2021;
14. Butt YM, Smith ML, Tazelaar HD, Roden AC, Mengoli MC, Larsen BT. Surgical Pathology of Diffuse Parenchymal Lung Disease in Patients with Psoriasis or Psoriatic Arthritis. Arch Pathol Lab Med. 2023;
15. Kazlouskaya Viktoryia, Collins Mary-Katharine. https://www.pathologyoutlines.com/topic/skinnontumorpsoriasis.html. 2021. Pathology Outlines - Psoriasis.
16. Olejniczak-Staruch I, Ciążyńska M, Sobolewska-Sztychny D, Narbutt J, Skibińska M, Lesiak A. Alterations of the skin and gut microbiome in psoriasis and psoriatic arthritis. Int J Mol Sci. 2021;
17. How KN, Yap WH, Lim CLH, Goh BH, Lai ZW. Hyaluronic Acid-Mediated Drug Delivery System Targeting for Inflammatory Skin Diseases: A Mini Review. Frontiers in Pharmacology. 2020.
18. He H, Bissonnette R, Wu J, Diaz A, Saint-Cyr Proulx E, Maari C, et al. Tape strips detect distinct immune and barrier profiles in atopic dermatitis and psoriasis. J Allergy Clin Immunol. 2021;
19. Ali MS, Alam MS, Imam FI, Siddiqui MR. Topical nanoemulsion of turmeric oil for psoriasis: Characterization, ex vivo and in vivo assessment. Int J Drug Deliv. 2012;
20. A. K, A. A, J. A, S. B. Conundrum and therapeutic potential of curcumin in drug delivery. Critical Reviews in Therapeutic Drug Carrier Systems. 2010.
21. Abdullahi1 A, Muhammad MT, Suleiman J, Sokoto1 RM. Isolation and Identification of Bacteria Associated with Aerial Part of Rice Plant from Kware Lake. Asian J Res Bot. 2018;
22. Ofori DA, Anjarwalla P, Mwaura L. ASUHAN KEPERAWATAN PADA PASIEN DENGAN GAGAL GINJAL KRONIS YANG DI RAWAT DI RUMAH SAKIT. Molecules. 2020;
23. Hekmatpou D, Mehrabi F, Rahzani K, Aminiyan A. The effect of aloe vera clinical trials on prevention and healing of skin wound: A systematic review. Iranian Journal of Medical Sciences. 2019.
24. Jales STL, Barbosa R de M, de Albuquerque AC, Duarte LHV, da Silva GR, Meirelles LMA, et al. Development and Characterization of Aloe vera Mucilaginous-Based Hydrogels for Psoriasis Treatment. J Compos Sci. 2022;
25. D. Dhangar P, Shimpi H, Newadkar R,

Bhadane V, Desale L, Jaiswal N. Formulation and Evaluation of Herbal Extract of Butterfly Pea Multipurpose Cream. Res J Top Cosmet Sci. 2023;
26. Hoffmann J, Gendrisch F, Schempp CM, Wölfle U. New herbal biomedicines for the topical treatment of dermatological disorders. Biomedicines. 2020.
27. Fadaei F, Ayati MH, Firooz A, Younespour S, Abouali M, Tabarrai M, et al. Efficacy of a Topical Herbal Cream Containing Frankincense Oil, Pumpkin Oil and Licorice Aqueous Extract in Patients with Mild-to-Moderate Plaque Psoriasis: a Randomized Clinical Trial. Res J Pharmacogn. 2022;
28. Togni S, Maramaldi G, Di Pierro F, Biondi M. A cosmeceutical formulation based on boswellic acids for the treatment of erythematous eczema and psoriasis. Clin Cosmet Investig Dermatol. 2014;
29. Lokhande S, Patil S, Parshurami S. EFFICACY OF PANCHATIKTA GHRIT GUGGUL IN THE MANAGEMENT OF MANDAL KUSHTHA WITH SPECIAL REFERENCE TO PSORIASIS. Int J Res Ayurveda Pharm. 2016;
30. Ernst E. Nutraceuticals: The Complete Encyclopedia of Supplements, Herbs, Vitamins, and Healing Foods. Focus Altern Complement Ther. 2001;
31. Reena K, Mittal S, Faizan M, Jahan I, Rahman Y, Khan R, et al. Enhancement of Curcumin's Anti-Psoriatic Efficacy via Formulation into Tea Tree Oil-Based Emulgel. Gels. 2023;
32. Sonia K, Anupama D. Microemulsion based transdermal drug delivery of tea tree oil. Int J Drug Dev Res. 2011;
33. IRCT20200115046143N1. Formulation and clinical evaluation of muccoadhesive gel containing licorice based nanoniosomes for treatment of oral ulcers. http://www.who.int/trialsearch/Trial2.aspx?TrialID=IRCT20200115046143N1. 2020;
34. Uva L, Miguel D, Pinheiro C, Antunes J, Cruz D, Ferreira J, et al. Mechanisms of action of topical corticosteroids in psoriasis. International Journal of Endocrinology. 2012.
35. Yadav K, Singh D, Singh MR. Development and characterization of corticosteroid loaded lipid carrier system for psoriasis. Res J Pharm Technol. 2021;
36. Fogh K, Kragballe K. New vitamin D analogs in psoriasis. Current Drug Targets: Inflammation and Allergy. 2004.
37. Sigmon JR, Yentzer BA, Feldman SR. Calcitriol ointment: A review of a topical vitamin D analog for psoriasis. Journal of Dermatological Treatment. 2009.
38. Kragballe K. Vitamin D analogues in the treatment of psoriasis. J Cell Biochem. 1992;
39. Jaiswal M, Dudhe R, Sharma PK. Nanoemulsion: an advanced mode of drug delivery system. 3 Biotech. 2015.
40. Latif MS, Nawaz A, Asmari M, Uddin J, Ullah H, Ahmad S. Formulation Development and In Vitro/In Vivo Characterization of Methotrexate-Loaded Nanoemulsion Gel Formulations for Enhanced Topical Delivery. Gels. 2023;
41. Sadeq ZA. Review on nanoemulsion: Preparation and evaluation. International Journal of Drug Delivery Technology. 2020.
42. Tripathi D, Srivastava M, Rathour K, Rai AK, Wal P, Sahoo J, et al. A Promising Approach of Dermal Targeting of Antipsoriatic Drugs via Engineered Nanocarriers Drug Delivery Systems for Tackling Psoriasis. Drug metabolism and bioanalysis letters. 2023.
43. Renstra kemenkes. Peraturan Menteri Kesehatan Repblik Indonesia No 21 Tahun 2020 Tentang Rencana Strategis Kemenentrian Kesehatan 2020-2024. Kemenkes. 2020;
44. Suliman RS, Ali H, Nurulain I, Shamiha NN, Nizam M, Budiasih S, et al. CINNAMON BARK EXTRACT FOR THE FORMULATION AND CHARACTERISATION OF ANTIMICROBIAL CREAM. Int J Res Ayurveda Pharm. 2017;
45. Rachmawati H, Budiputra DK, Mauludin R. Curcumin nanoemulsion for transdermal application: Formulation and evaluation. Drug Dev Ind Pharm. 2015;
46. Nemattalab M, Rohani M, Evazalipour M, Hesari Z. Formulation of Cinnamon

(Cinnamomum verum) oil loaded solid lipid nanoparticles and evaluation of its antibacterial activity against Multi-drug Resistant Escherichia coli. BMC Complement Med Ther. 2022;

47. Tanzidi-Roodi O, Jafari F, AkbariRad M, Asili J, Elyasi S. Evaluation of a new herbal formulation (Viabet®) efficacy in patients with type 2 diabetes as an adjuvant to metformin: A randomized, triple-blind, placebo-controlled clinical trial. J Herb Med. 2023;
48. Choobkar N, Daraei Garmakhany A, Aghajani AR, Ataee M. Response surface optimization of pudding formulation containing fish gelatin and clove (Syzygium aromaticum) and cinnamon (Cinnamomum verum) powder: Effect on color, physicochemical, and sensory attributes of the final pudding product. Food Sci Nutr. 2022;
49. Iyer MS, Gujjari AK, Paranthaman S, Lila ASA, Almansour K, Alshammari F, et al. Development and Evaluation of Clove and Cinnamon Supercritical Fluid Extracts-Loaded Emulgel for Antifungal Activity in Denture Stomatitis. Gels. 2022;
50. Ullah N, Amin A, Farid A, Selim S, Rashid SA, Aziz MI, et al. Development and Evaluation of Essential Oil-Based Nanoemulgel Formulation for the Treatment of Oral Bacterial Infections. Gels. 2023;
51. Pimpale A. Formulation and Evaluation of Antibacterial, Antifungal Cream of Garlic Oil. Int J Trend Sci Res Dev. 2018;
52. Hassanzadeh H, Rahbari M, Galali Y, Hosseini M, Ghanbarzadeh B. The garlic extract-loaded nanoemulsion: Study of physicochemical, rheological, and antimicrobial properties and its application in mayonnaise. Food Sci Nutr. 2023;
53. Orugun OA, Uronnachi EM, Issac J, Yahaya ZS, Nnamani ND. Formulation and in vitro trypanocidal evaluation of garlic oil nanoemulsions. J Res Pharm. 2023;
54. Almehmady AM, Ali SA. Transdermal film loaded with garlic oil-acyclovir nanoemulsion to overcome barriers for its use in alleviating cold sore conditions. Pharmaceutics. 2021;
55. Al-Shaibani AJN, Al-Gburib KMH, Hamraha KTKA, Alridhab AMA. Design and characterization of candesartan cilexetil oral nanoemulsion containing garlic oil. Int J Appl Pharm. 2019;
56. Dabodhia KL, Lamba NP, Manchanda S, Chauhan MS. Formulation and Evaluation of Synergistic effect of Garlic Oil and D-Limonene Nanoemulsion for its Anti-fungal Properties Against Tomato Leaf Spot Disease. Orient J Chem. 2022;
57. Youssef AAA, Cai C, Dudhipala N, Majumdar S. Design of topical ocular ciprofloxacin nanoemulsion for the management of bacterial keratitis. Pharmaceuticals. 2021;
58. Younis MK, Khalil IA, Younis NS, Fakhr Eldeen RR, Abdelnaby RM, Aldeeb RA, et al. Aceclofenac/Citronellol Oil Nanoemulsion Repurposing Study: Formulation, In Vitro Characterization, and In Silico Evaluation of Their Antiproliferative and Pro-Apoptotic Activity against Melanoma Cell Line. Biomedicines. 2023;
59. Jurišić Dukovski B, Juretić M, Bračko D, Randjelović D, Savić S, Crespo Moral M, et al. Functional ibuprofen-loaded cationic nanoemulsion: Development and optimization for dry eye disease treatment. Int J Pharm. 2020;
60. Makhmalzadeh BS, Torabi S, Azarpanah A. Optimization of Ibuprofen delivery through rat skin from traditional and novel nanoemulsion formulations. Iran J Pharm Res. 2012;
61. Chen CY, Tsai TY, Chen BH. Effects of black garlic extract and nanoemulsion on the deoxy corticosterone acetate-salt induced hypertension and its associated mild cognitive impairment in rats. Antioxidants. 2021;
62. Osonwa UE, Okechukwu SA, Ihekwereme CP, Chukwu KI, Eluu SC, Azevedo RB. Formulation and evaluation of therapeutic potential of nanoemulsion of a blend of antimicrobial oils. Trop J Nat Prod Res. 2018;
63. Ragavan G, Muralidaran Y, Sridharan B, Nachiappa Ganesh R, Viswanathan P. Evaluation of garlic oil in nano-emulsified

form: Optimization and its efficacy in high-fat diet induced dyslipidemia in Wistar rats. Food Chem Toxicol. 2017;

64. Choupanian M, Omar D, Basri M, Asib N. Preparation and characterization of neem oil nanoemulsion formulations against Sitophilus oryzae and Tribolium castaneum adults. J Pestic Sci. 2017;
65. Reddy JP, Rhim JW. Extraction and Characterization of Cellulose Microfibers from Agricultural Wastes of Onion and Garlic. J Nat Fibers. 2018;
66. Mondéjar-López M, Rubio-Moraga A, López-Jimenez AJ, García Martínez JC, Ahrazem O, Gómez-Gómez L, et al. Chitosan nanoparticles loaded with garlic essential oil: A new alternative to tebuconazole as seed dressing agent. Carbohydr Polym. 2022;
67. Booyens J, Thantsha MS. Fourier transform infra-red spectroscopy and flow cytometric assessment of the antibacterial mechanism of action of aqueous extract of garlic (Allium sativum) against selected probiotic Bifidobacterium strains. BMC Complement Altern Med. 2014;
68. EN 1991-1-4. Eurocode 1: Actions on structures -Part 1-4: General actions -Wind actions. Eur Comm Stand. 2005;
69. Chandira Rm, Gracy Gladin S, Chandira M. Formulation and Evaluation of Herbal Soap by using Melt and Pour Method. Indian J Nat Sci www.tnsroindia.org.in ©IJONS. 2022;
70. Abdallah MH, Elghamry HA, Khalifa NE, Khojali WMA, Khafagy ES, Shawky S, et al. Development and Optimization of Erythromycin Loaded Transethosomes Cinnamon Oil Based Emulgel for Antimicrobial Efficiency. Gels. 2023;
71. Hosny KM, Khallaf RA, Asfour HZ, Rizg WY, Alhakamy NA, Sindi AM, et al. Development and optimization of cinnamon oil nanoemulgel for enhancement of solubility and evaluation of antibacterial, antifungal and analgesic effects against oral microbiota. Pharmaceutics. 2021;
72. Duangjit S, Rattanachithawat N, Opanasopit P, Ngawhirunpat T. Development and optimization of finasteride-cinnamon oil-loaded ethanol-free microemulsions for transdermal delivery. J Drug Deliv Sci Technol. 2022;
73. Rajkovic K, Pekmezovic M, Barac A, Nikodinovic-Runic J, Arsić Arsenijević V. Inhibitory effect of thyme and cinnamon essential oils on Aspergillus flavus: Optimization and activity prediction model development. Ind Crops Prod. 2015;
74. Abd El Wahab LM, Essa EA, El Maghraby GM, Arafa MF. The Development and Evaluation of Phase Transition Microemulsion for Ocular Delivery of Acetazolamide for Glaucoma Treatment. AAPS PharmSciTech. 2023;
75. Li YJ, Hu X Bin, Lu XL, Liao DH, Tang TT, Wu JY, et al. Nanoemulsion-based delivery system for enhanced oral bioavailability and caco-2 cell monolayers permeability of berberine hydrochloride. Drug Deliv. 2017;
76. Peng C, Svirskis D, Lee SJ, Oey I, Kwak HS, Chen G, et al. Design of microemulsion system suitable for the oral delivery of poorly aqueous soluble beta-carotene. Pharm Dev Technol. 2018;
77. Yang X, Gao P, Jiang Z, Luo Q, Mu C, Cui M. Preparation and Evaluation of Self-emulsifying Drug Delivery System (SEDDS) of Cepharanthine. AAPS PharmSciTech. 2021;
78. Sodalee K, Sapsuphan P, Wongsirikul R, Puttipipatkhachorn S. Preparation and evaluation of alpha-mangostin solid self-emulsifying drug delivery system. Asian J Pharm Sci. 2016;
79. Aziz A, Zaman M, Khan MA, Jamshaid T, Butt MH, Hameed H, et al. Preparation and Evaluation of a Self-Emulsifying Drug Delivery System for Improving the Solubility and Permeability of Ticagrelor. ACS Omega. 2024;
80. Wannas AN, Abdul-Hasan MT, Jawad KKM, Razzaq IFA. PREPARATION AND IN VITRO EVALUATION OF SELF-NANO EMULSIFYING DRUG DELIVERY SYSTEMS OF KETOPROFEN. Int J Appl Pharm. 2023;
81. Li F, Song S, Guo Y, Zhao Q, Zhang X, Pan W, et al. Preparation and pharmacokinetics evaluation of oral self-emulsifying system

for poorly water-soluble drug Lornoxicam. Drug Deliv. 2015;

82. Ujhelyi Z, Vecsernyés M, Fehér P, Kósa D, Arany P, Nemes D, et al. Physico-chemical characterization of self-emulsifying drug delivery systems. Drug Discovery Today: Technologies. 2018.
83. Patil P, Joshi P, Paradkar A. Effect of formulation variables on preparation and evaluation of gelled self-emulsifying drug delivery system (SEDDS) of ketoprofen. AAPS PharmSciTech. 2004;
84. Teja PK, Mithiya J, Kate AS, Bairwa K, Chauthe SK. Herbal nanomedicines: Recent advancements, challenges, opportunities and regulatory overview. Phytomedicine. 2022;
85. d A, M N. Preparation and In Vitro Evaluation of Self-Emulsifying Drug Delivery System for Oral Delivery of Glibenclamide. Int J Pharm Pharmacol. 2017;
86. Hussain A, Samad A, Singh SK, Ahsan MN, Haque MW, Faruk A, et al. Nanoemulsion gel-based topical delivery of an antifungal drug: In vitro activity and in vivo evaluation. Drug Deliv. 2016;
87. Lakshmi Usha Ayalasomayajula. AN UPDATE ON RECENT ADVANCES IN NANOEMULSION BASED HYDROGELS: NANOEMULGELS. J Pharm Negat Results. 2023;
88. Basera K. Nanoemulgel: a Novel Formulation Approach for Topical Deliverey of Hydrophobic Drugs. Basera al World J Pharm Pharm Sci. 2015;
89. Gupta R, Garg T, Sharma RB. Preparation and Characterization of Luliconazole Nanoemulsion Based Hydrogel. Int J Pharm Sci Med. 2022;
90. Elosaily GH, Salem HA, Hassan AM, Maxwell S, Ibrahim ZA.) Formulation, In-vitro and In-vivo Evaluation of Nystatin Topical Gel. Journal of American Science. 2014.
91. Mokarizadeh M, Kafil H, Ghanbarzadeh S, Alizadeh A, Hamishehkar H. Improvement of citral antimicrobial activity by incorporation into nanostructured lipid carriers: A potential application in food stuffs as a natural preservative. Res Pharm Sci. 2017;
92. Orswant C, Hore PET, Chatzidaki MD, Mateos-Diaz E, Leal-calderon F, Xenakis A, et al. Triglyceride-Based Microemulsion for Intravenous Administration of. An Acad Bras Cienc. 2016;

*****